Neutron diffraction study of gallium nanostructured within a porous glass

Y. A. Kibalin* and I. V. Golosovsky
Petersburg Nuclear Physics Institute, 188300, Gatchina, Russia

Y. A. Kumzerov
Ioffe Physical Technical Institute, 194021, St. Petersburg, Russia

V. Y. Pomjakushin
Paul Scherrer Institute, 5232, Villigen, Switzerland

A. A. Bosak
European Synchrotron Radiation Facility, Box Post 220, F-38043, Grenoble, Cedex, France

P. P. Parshin
National Research Centre "Kurchatov Institute," 123182, Moscow, Russia
(Received 13 April 2012; published 16 July 2012)

Neutron diffraction studies of structure and atomic vibrations in gallium nanoparticles with the size of 13 nm embedded into a porous glass were performed. At crystallization of gallium, which at room temperature is in a liquid state, the texture effects were observed. The modeling of texture by generalized spherical harmonics allowed us to measure the temperature dependence of the mean-square displacement. It was shown that the contribution of acoustic vibrations in the phonon spectrum of conned gallium is dominant. The Debye temperature of nanostructured gallium appeared to be close to that for the bulk. The Grüneisen constant was found to be strongly reduced with respect to the bulk, as well as the thermal expansion coefficient. It was demonstrated that texture affects physical properties, in particular, superconductivity through inner stresses.

DOI: 10.1103/PhysRevB.86.024302 PACS number(s): 61.05.fm, 63.22.Kn

I. INTRODUCTION

Atomic motion determines fundamental macroscopic properties of condensed matter such as thermal conductivity, thermal expansion, and others. Therefore, atomic vibrations in nanoparticles embedded within porous host matrices attract great interest, taking into consideration the potential opportunities for a practical application. These nanoparticles are under the so-called conditions of "confined geometry" and demonstrate unusual physical properties. They are caused by several fundamental reasons: The size of nanoparticles is comparable with the characteristic lengths of interactions and the number of atoms at the surface of a nanoparticle is comparable to its total number of atoms. Note that physical properties of nanoparticles within a porous matrix are strongly influenced by the interaction between particles and the matrix.

Low-melting metals such as Ga, Bi, Pb, and others possess a large amplitude of atomic vibrations and are attractive for studies of atomic motion. Moreover, the developed technology of embedding nanoparticles into a porous glass from melt under an external pressure allows us to produce nanoparticles with a small size dispersion. The average dimension of nanoparticles can range from 6 up to 40 nm, depending on the glass characteristics and conditions of the synthesis.

To our knowledge, there are only a few studies of atomic motion in low-melting metal nanoparticles by elastic neutron scattering through measurements of atomic thermal factor[1–4] and density of phonon states via inelastic neutron scattering.[5–8] This state of research is caused by the difficulty in the preparation of a sufficient amount of a sample for neutron diffraction. Since this quantity is usually small and diffraction peaks are strongly broadened because of size effects, the registered signal is very weak. Apart from neutron diffraction, last year's other experimental methods such as synchrotron Mössbauer spectroscopy were started to probe the phonon density of states in nanomaterials.[8] However, due to the multiphonon processes, such measurements are usually carried out at low temperatures only.

The present paper continues the investigations by neutron diffraction. We report on the results of neutron diffraction studies of gallium nanostructured within a porous glass over a wide temperature range.

Among low-melting metals, gallium attracts particular attention. Bulk gallium crystallizes in eight different modifications of which only the orthorhombic one, known as α phase with the space group *Cmca*, is stable under ambient conditions.[9] Nanostructured gallium has different crystalline modifications as well, crystal structures for some of them have not been identified yet.[10–18] It should be noted that in the bulk only the orthorhombic α phase is stable. Others can be observed solely under special conditions. Moreover, gallium expands during solidification within pores; that creates additional stresses, which affect its physical properties.

Finally, at helium temperatures, gallium undergoes a transition into a superconducting state. The coherence length (the size of Cooper pair) for the bulk gallium is more than 160 nm.[19] Although the coherence length is much larger than the size of gallium nanoparticles within a porous glass, 14–15 nm, a sharp superconducting transition was observed at low temperatures.[10,20,21] The samples with different pore sizes and, consequently, with different sizes of the embedded

nanoparticles were studied. It was shown that in the samples with the pore size of 7 nm there is a gradual superconducting transition, whereas for other samples the transition was sharp.[11]

The large discrepancy in the reported results initiated the neutron diffraction studies of gallium nanostructured within a porous glass with the pore size of 7 nm. In diffraction the amplitude of atomic vibrations can be revealed by an atomic temperature factor (Debye-Waller factor), which is the Fourier transform of the probability density to find an atom at a certain distance from an equilibrium position.

II. EXPERIMENT

The porous vycor™-type glass with a random network of elongated pores was used as a host matrix.[22] The volume fraction of pores was about 20%; their mean diameter was 7 nm with a dispersion of a few percent.

The amorphous quartz (silica), which composes the body of the matrix, does not give any Bragg reflections. Therefore, the coherent scattering from the embedded objects can be easily separated from the diffuse scattering from the amorphous matrix. Since the silica is chemically inert and has a high-melting point, there is a possibility to synthesize the metallic nanoparticles into the pores from the melt under the external pressure of 10–15 kbar. After reaching the desired pressure, the temperature is slowly decreased and the metal starts to crystallize. In this technique, up to 90% of the pore volume is occupied by metal.

The diffraction experiments were performed on the diffractometer HRPT (Paul-Scherrer Institute, Switzerland) with the wavelength of 1.494 Å using a standard "orange cryostat" with vertical loading. The sample had a form of parallelepiped with the dimensions of $4 \times 5 \times 12$ mm.[23]

At room temperature, gallium within the pores is in a liquid state. The crystallization occurs during cooling about 240–280 K in the cryostat chamber. To determine the effect of crystallization conditions on the structure and the morphology of the gallium nanoparticles, we performed experiments with different cooling rates. In a typical experiment, the sample was cooled to 2 K with a cooling rate of 2 K/min. The successive measurements of neutron diffraction were carried out with heating from 2 K to room temperature.

III. RESULTS AND DISCUSSION

Unexpectedly, the diffraction measurements demonstrated a strong texture since the intensities of the reflections varied with sample orientation (Fig. 1). Moreover, the intensities varied with temperature, unlike the normal dependence due to the temperature factor. It is rather surprising, as the previous structural studies of the nanostructured lead and selenium[1,2] showed that the powder averaging is well accomplished.

In principle, the incomplete powder averaging is possible if the sample consists of randomly oriented large (in order of microns) crystallites. However, the size of the embedded particles, defined from the peak broadening, was estimated to be 130–140 Å. It should be stressed that the porous glass cannot be responsible for the appearance of the texture, because the pores are oriented randomly.

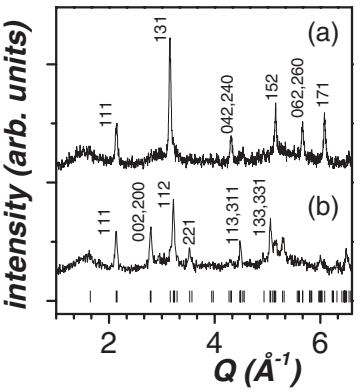

FIG. 1. Neutron diffraction patterns measured at 2 K for two orientations of the sample, differing by 30 deg.

Since the texture is much more pronounced for fast cooled samples, the possible reason for the texture could be a presence of temperature gradients. These nonuniform fields can initiate a preferable orientation of the crystallites during the crystallization. Gallium is a highly anisotropic material,[24] which gives strong evidence for such a scenario.

Thus, in order to describe the neutron diffraction pattern and to acquire the Debye-Waller factors, we have to describe the texture.

A. Texture

In general, the orientation of a certain crystallite is determined by the orientation of its coordinate system K_C with respect to the laboratory coordinate system K_L. These coordinate systems are related by

$$K_C = g \cdot K_L, \tag{1}$$

where g is the orientation matrix.

Let us denote the probability for a crystallite to be oriented in the direction defined by the matrix g as $f(g)$-orientation distribution function. Then the intensity of a diffraction reflection hkl can be written as[25]

$$I_{hkl} = \frac{N_{hkl}}{2\pi} \int_{(hkl)} f(g) dg. \tag{2}$$

The integration is performed over all crystallites, which are oriented in the reflecting position hkl. The coefficient N_{hkl} determines other factors affecting intensity: Structural factor, temperature factor, Lorentz factor, absorption, etc.

It is convenient to model the orientation distribution function $f(g)$ by spherical harmonic expansion[25]:

$$f(g) = \sum_{l=0}^{l_{\max}} \sum_{m=-l}^{l} \sum_{n=-l}^{l} C_l^{mn} T_l^{mn}(g). \tag{3}$$

The weighting factors C_l^{mn} are considered variable parameters during the diffraction pattern fitting. For centrosymmetric crystals, the series (3) contains terms with even l only.[26]

The texture effects are usually described by the projection of the reflection sphere "density" of a certain reflection in the equatorial plane. Such projections are well known as the "pole figures." We used for evaluation of the texture effects the simpler integral parameter, known as the texture index F_2

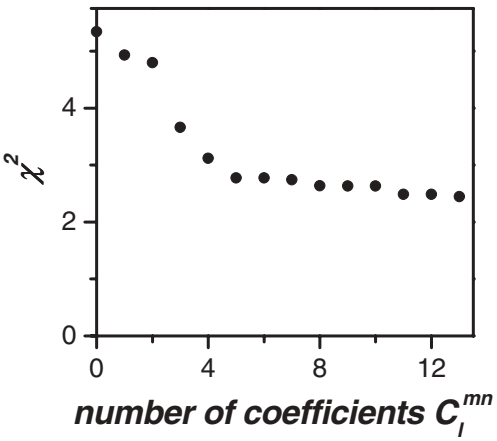

FIG. 2. The dependence of the convergence factor χ^2 vs the number of spherical harmonics used in an approximation.

(Ref. 25):

$$F_2 = \int f^2(g)dg. \tag{4}$$

Here the integral is taken over all possible crystallite orientations. For an ideal powder $F_2 = 1$, while for another limit case a single crystal $F_2 = \infty$. In the spherical harmonic expansion the texture index can be expressed as

$$F_2 = 1 + \sum_{l=2}^{l_{\max}} \frac{1}{2l+1} \sum_{m=-l}^{l} \sum_{n=-l}^{l} C_l^{mn}. \tag{5}$$

In refinements of the neutron diffraction patterns by the Rietveld method[27] we used the MAUD code, where the spherical harmonic expansion was carried out.[28] In Fig. 2 the dependence of the convergence factor χ^2 on the number of harmonics used in refinement is shown. It can be seen that 5–6 harmonics are enough for an adequate description. An example of profile analysis of a neutron diffraction pattern is shown in Fig. 3.

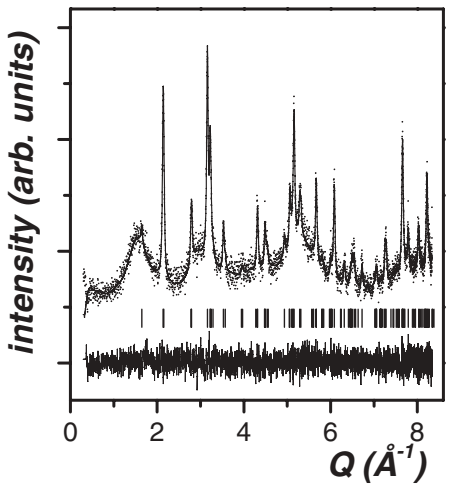

FIG. 3. Profile analysis of the neutron diffraction pattern measured at 2 K after slow cooling of the sample. The row of bars marks the positions of Bragg reflections. Below is the difference between the measured and calculated profiles.

The texture effects strongly depend on a cooling rate. In particular, fast cooled samples exhibit very strong texture, which cannot be described reliably. Here, for a correct description, a large number of the spherical harmonics is needed. It leads to an increasing number of variable parameters, which become bigger than the number of observed reflections.

Note that the texture effects in gallium nanoparticles had also been observed before, although they were not identified in these terms. It was reported that at crystallization of gallium in nanotubes with the diameter of about 100 Å, the Ga nanocrystals are always oriented in the same way with respect to the nanotube axis.[17]

B. Temperature evolution of morphology, structure, and texture

Peak broadenings corrected for instrumental resolution originate from the size effect and inner stresses. In the first case, the peak broadening does not depend on reciprocal lattice vectors, while, in the second case, it is proportional to momentum transfer. Therefore, the contributions from the size effect and inner stresses can be distinguished.

The size of the nanoparticles is about 13.0–13.5 nm[47] and appears to be temperature independent except for low temperatures, where a slight decrease with temperature can be seen [Fig. 4(a)]. However, the inner stresses demonstrate a sharp dependence, they practically disappear above 5 K [Fig. 4(b)].

In calculations the pseudo-Voigt line shape, known as the Thompson-Cox-Gastings approximation, was used.[29]

There are some reports about different crystal structures of the nanostructured gallium: Monoclinic,[16,17] hexagonal,[16] and tetragonal[18] at freezing. However, in our neutron diffraction experiments at all cooling rates, the reflections from the nanostructured gallium were indexed with the centrosymmetric orthorhombic space group *Cmca*, which corresponds to the known α phase[9] with eight atoms at the unit cell. The unit

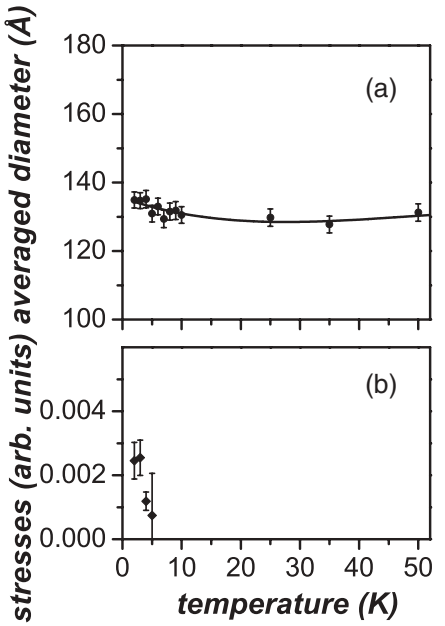

FIG. 4. The temperature dependence of the volume averaged nanoparticle size (a) and the inner stresses (b).

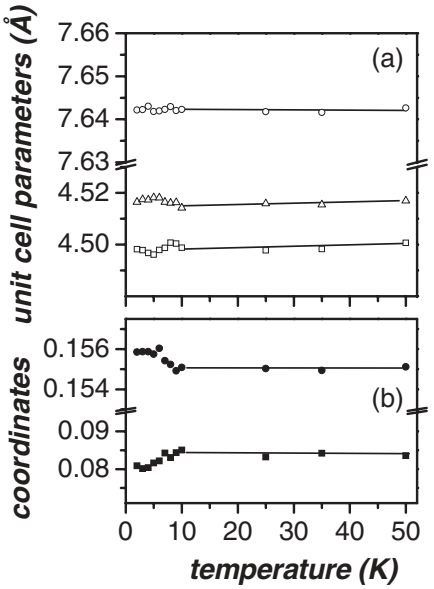

FIG. 5. The temperature dependence of the unit cell parameters a (squares), b (circles), and c (triangles) (top panel). y (circles) and z projection (squares) of the Ga atom coordinate (bottom panel). The experimental errors do not exceed the symbol size if not shown.

cell parameters of the nanostructured gallium at 250 K were refined as follow: $a = 0.4513(2)$ nm, $b = 0.7654(1)$ nm, and $c = 0.4523(1)$ nm. They are similar to those reported for the bulk.

The temperature dependencies of the unit cell parameters and atomic coordinate of the Ga atom are shown in Fig. 5. Above 50 K the temperature dependence does not show any features. However, at low temperatures, some anomalies are clearly seen. Apparently at temperatures below 10 K, gallium undergoes structural changes: The z coordinate of the Ga atom decreases, whereas the y coordinate increases on cooling. It corresponds to a rotation of dimers comprised from nearest pairs of atoms, while the size of the dimers remains constant. The correlation of the structure parameters with the stresses, estimated from the peak broadening, and a texture is clearly visible [see Figs. 5(b) and 6].

The texture index displays an abrupt decrease at low temperatures as well (Fig. 6). It means that the strong

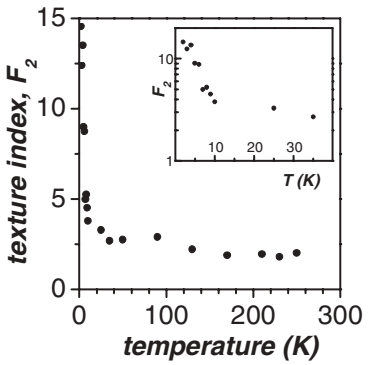

FIG. 6. Temperature dependence of the texture index. The texture index in the low temperature range is shown in an inset. The experimental errors do not exceed the symbol size if not shown.

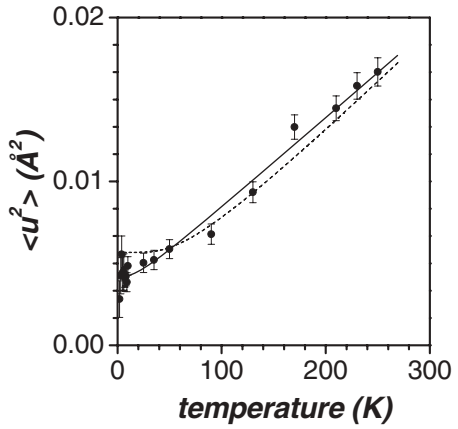

FIG. 7. Isotropic mean-square displacement vs temperature for confined Ga. Solid line is a fit by the Debye model, dotted line is a fit by the Einstein model.

texture, which appeared at solidification rapidly, relaxes with increasing temperature. It looks like the inner stresses are related to the texture.

C. Atomic motion in confined Ga

The effect of atomic thermal vibrations on the intensity of Bragg reflections is described by the temperature factor $T_k(\mathbf{Q})$, which, in the approximation of the independent normal modes, can be written as

$$T_k(\mathbf{Q}) = \exp\left[-\frac{1}{2}\langle(\mathbf{Q}\cdot\mathbf{u}_k)^2\rangle\right], \tag{6}$$

here $\mathbf{Q}$ is momentum transfer and $\mathbf{u}_k$ is the displacement of the k atom from its equilibrium position. In an isotropic case, the atomic motion is expressed by the isotropic Debye-Waller factor B:

$$B = 8\pi^2\langle u^2\rangle. \tag{7}$$

Then the atomic temperature factor reduces to

$$T_{\rm iso}(Q) = \exp\left(-B\frac{Q^2}{16\pi^2}\right). \tag{8}$$

The temperature dependence of the mean-square displacement $\langle u^2\rangle$, calculated from the refined Debye-Waller factors, is shown in Fig. 7. A relatively high value of the temperature independent constant mean-square displacement shows a weak binding among atoms that should be attributed to a high density of defects which is typical for nanostructured objects.

As well known, the temperature dependence of $\langle u^2\rangle$ can be described by the Debye or the Einstein model.[30] The Debye model ignores optical branches, while in the Einstein model only optical vibrations are considered. It appears that the temperature dependence is well approximated by the Debye model:

$$\langle u^2\rangle = \frac{3\hbar^2 T}{mk_B\Theta_D^2}\left[\frac{T}{\Theta_D}\int_0^{\frac{\Theta_D}{T}}\frac{x}{\exp(x)-1}\,dx + \frac{\Theta_D}{4T}\right] + \langle u_0^2\rangle, \tag{9}$$

with parameters $\Theta_D = 185(3)$ K and the static contribution $\langle u_0^2\rangle = 0.0015(2)$ Å^2. The approximation based on the Einstein

model is worse, the value χ^2, which defines the goodness-of-fit, is larger by five times. In Fig. 7 it can be seen that the deviation from the Einstein model occurs mainly at low temperatures. Better agreement of experimental data with the Debye model shows that the contribution of the acoustic vibrations in the phonon spectrum of nanostructured gallium is dominant.

It is interesting that x-ray diffraction measurements on bulk gallium[31] demonstrate the Debye temperature of 189(6) K, which is close to that measured for nanostructured Ga within a porous glass in our case. Moreover, analysis of literature data shows that the Debye temperature measured from the low temperature specific heat in the nanostructured gallium[32] and in the bulk[33] appear to be very close too: 300 and 325(2) K, respectively. The difference of the specific heat and diffraction Debye temperatures arises from the different averaging among the velocities of longitudinal and transverse phonons. It was shown that in the classical limit specific-heat Debye temperature should be $\sqrt{Z}$ times larger than diffraction Debye temperature, where Z is the number of atoms in the unit cell.[34]

The proximity of the Debye temperatures for nanoparticles and for the bulk measured by different methods means that the density of phonon states does not undergo significant changes at low frequencies. It should be noted that for the liquid gallium within a porous glass the situation is opposite—the density of phonon states is reduced at low frequencies in comparison to the bulk.[5,35]

The similar closeness of Debye temperatures in the embedded nanoparticles of Se and in the bulk were reported.[2] However, for Pb within a porous glass, the decrease of specific-heat Debye temperature with respect to the bulk was claimed.[36] That agrees to the increase in the density of phonon states at low energies as observed experimentally.[7]

It is well known that anharmonicity plays an important role in the thermal motion of atoms. Unfortunately, in our case, an accuracy of the refined mean-square displacement is not enough to see the anharmonic effects. However, the anharmonicity of atomic vibrations determines thermal expansion, which can be calculated from the temperature dependence of unit cell parameters (Fig. 8).

In the first approximation, this dependence, obtained from the classical Mie-Grüneisen equation, can be written as follows[37,38]:

$$V(T) = V_0 + \frac{\gamma}{c}E(T), \tag{10}$$

here V_0 is the molar volume, c is the elastic modulus, γ is the Grüneisen constant, and $E(T)$ is the thermal energy. In the Debye model the thermal energy at temperature T is determined as follows:

$$E(\Theta_D,T) = 9N_A k_B \frac{T^4}{\Theta_D^3}\int_0^{\frac{\Theta_D}{T}} \frac{x^3}{\exp(x)-1}\,dx. \tag{11}$$

Here N_A is the Avogadro's number, k_B is the Boltzmann constant, and Θ_D is the Debye temperature.

The fit of $V(T)$ according to Eq. (10) gives $c/\gamma = 64(3)$ GPa at fixed $\Theta_D = 185$ K, found from $\langle u(T)^2\rangle$. In the Debye model the elastic modulus c is proportional to the square of Θ_D.[39] Therefore, taking into account the known values of the Debye temperature for the bulk and the nanostructured gallium and the elastic modulus of bulk gallium of 61.3 GPa,[40] one can estimate the elastic modulus of the nanostructured gallium as 59(3) GPa and, consequently, $\gamma = 0.92(6)$.

For most ordinary metals the Grüneisen constant γ takes values from 0.8 to 3. For example, in bismuth it equals 1.2, in lead 2.63. Since $\gamma = 1.5$ in the bulk gallium,[41,42] the nanostructured gallium value appears to be strongly reduced. The similar decreasing of the Grüneisen constant was observed in diffraction studies of the lead nanostructured within a porous glass.[1]

The smaller magnitude of γ is consistent with the lower thermal expansion coefficient (TEC) of gallium embedded within a porous glass with respect to the bulk.[43,44] These dependencies are shown in the inset in Fig. 8. The TEC for nanostructured Ga is calculated from the fitting of the thermal dependence of the unit cell volume according to Eq. (10).

IV. PHYSICAL PROPERTIES AND TEXTURE

Despite a strong influence of texture on the physical properties of gallium within a porous glass, our diffraction experiments demonstrated that at 270 K Ga is in a crystallized state in all cases, while at 290 K it is in a liquid state. It is consistent with the results from Ref. 14.

There are some general peculiarities, which are independent of the cooling rate. In particular, the observed sharp change in texture in the temperature range 5–7 K does not depend on the cooling rate. This means that the specific temperature range cannot be a characteristic of the embedded nanoparticle. In the inset in Fig. 8, it can be seen that at low temperatures the TEC of the nanostructured gallium is close to zero, in any case it is less than 3×10^{-7} K^{-1}.

To our knowledge, there are no experimental measurements of the TEC for a porous glass at low temperatures. However, from the approximation of the diffuse scattering due to the porous silica glass by the sum of Debye-like functions,[48] one can estimate Si-O and O-O distances of the tetrahedra

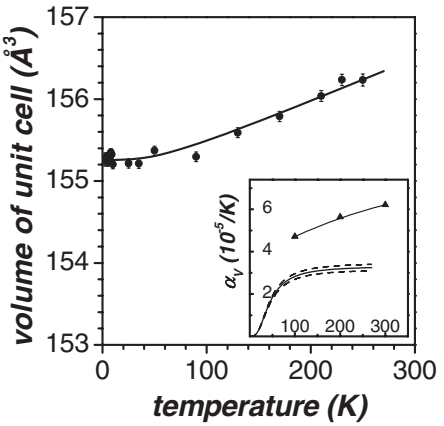

FIG. 8. The temperature dependence of the unit cell volume for nanostructured gallium. In the inset the thermal expansion coefficient for the nanostructured gallium calculated from the model fitting of the thermal dependence of the unit cell volume by Eq. (10) (solid line, dotted lines—confidence interval) and literature data for the bulk (solid circles) are shown.[43,44]

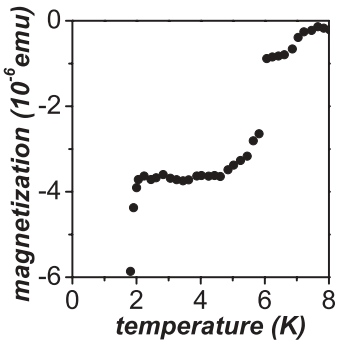

FIG. 9. ZFC magnetization vs temperature for the sample of gallium nanostructured in 7 nm porous glass. Reproduced from a paper by Charnaya *et al.*[12]

constituting silica. It was found that these distances are practically temperature independent. Since the TEC of the porous vycor-type glass at room temperature is about 7–8 $\times$ 10^{-7} K^{-1},[45] it is very plausible that the TEC of a porous glass is comparable with the TEC of gallium nanoparticles at helium temperatures. In this case, the observed effects at low temperatures, a sharp texture change, disappearance of the inner stresses, and structural transformation in the embedded gallium nanoparticles should be attributed to mechanical interactions between nanoparticles and a glass host matrix due to the difference in TEC. Similar effects were observed in the confined Se^2 and maghemite.[46]

In the bulk gallium, a sharp superconducting transition appears at 1.08 K. However, in gallium within a porous glass with the pore size of 7 nm, a smeared superconducting transition was observed[11,12] (see Fig. 9). With decreasing temperature, a diamagnetic behavior occurred at 6.2 K, whereas the complete superconductivity was aroused at 2.5 K. The samples used in these experiments were very close by technology of preparing those studied in our experiments. Therefore, we believe that the observed spreaded superconducting transition could be explained by the structural transformation at low temperatures since a similar effect was observed in our diffraction experiments.

Moreover, the increase of the superconducting transition temperature for confined nanoparticles, respectively the bulk, could be easily explained by the inner stresses. Indeed, in the model of the granular superconductor comprised of grains connected by the Josephson junctions,[10,11,20,21] the superconductivity should strongly depend on the strains, which directly affect the contacts. The differences in texture and inner stresses may explain the different behavior of the superconducting transition reported for the samples with different pore size.[11]

V. CONCLUSION

By neutron diffraction it was shown that nanoparticles of gallium with the sizes of 13–13.5 nm synthesized within a porous glass with the pore size of 7 nm possess unusual properties. At room temperature, gallium in pores is in a liquid state, therefore, at crystallization, a texture appears, which depends on the cooling rate of the sample and which affects the physical properties.

For heating the texture index decreases sharply in the temperature range 5–10 K. There the internal stresses, detected at the lowest temperatures, disappear. These effects are explained by a mechanical interaction between the nanoparticles and the glass matrix associated with the difference in thermal expansion coefficients of gallium and glass.

The modeling of texture by spherical harmonic expansion allowed us to measure the temperature dependence of the mean-square displacement. The approximation of this dependence by the Debye and the Einstein models indicates that the contribution of acoustic vibrations in the phonon spectrum of nanostructured gallium is dominant. The Debye temperature of nanostructured gallium appeared to be close to that for the bulk. It means that the density of phonon states does not undergo significant changes at low frequencies.

The anharmonic effects in the nanostructured gallium appeared to be strong. The Grüneisen constant for nanostructured gallium, acquired from the temperature dependence of the unit cell volume, was found strongly reduced with respect to the bulk that is consistent with the lower coefficient of thermal expansion of the embedded gallium in comparison to the bulk.

ACKNOWLEDGMENTS

This work was partially supported by the Grants RFBR-10-02-00576 and MESRF-16.518.11.7034. The authors thank Dr. A. I. Sokolov, Dr. S. Matthies, and Dr. S. L. Ginzburg for valuable discussions and critical comments. I.V.G. is grateful for financial support from AGAUR (project 2010-VIP-00096) and EC (FP7-2009-IRSES-247518).

*yurikibalin@gmail.com.

[1] I. V. Golosovsky, R. G. Delaplane, A. A. Naberezhnov, and Y. A. Kumzerov, Phys. Rev. B **69**, 132301 (2004).

[2] I. V. Golosovsky, O. P. Smirnov, R. G. Delaplane, A. Wannberg, Y. A. Kibalin, A. A. Naberezhnov, and S. B. Vakhrushev, Eur. Phys. J. B **54**, 211 (2006).

[3] Yu. A. Kibalin, I. V. Golosovsky, Yu. A. Kumzerov, and G. Andre, Sci. Tech. . SPbSPU (Russia) **94**, 59 (2010).

[4] A. V. Fokin, Yu. A. Kumzerov, N. M. Okuneva, A. A. Naberezhnov, S. B. Vakhrushev, I. V. Golosovsky, and A. I. Kurbakov, Phys. Rev. Lett. **89**, 175503 (2002).

[5] V. N. Bogomolov, N. A. Klushin, N. M. Okuneva, E. L. Plachenova, V. I. Pogrebnoi, and F. A. Chudnovsky, Fiz. Tverd. Tela (Leningrad): Sov. Phys. Solid State **13**, 1499 (1971).

[6] V. N. Bogomolov and N. A. Klushin, Fiz. Tverd. Tela (Leningrad): Sov. Phys. Solid State **15**, 514 (1973).

[7] P. P. Parshin, M. G. Zemlyanov, G. Kh. Panov, A. A. Shikov, A. A. Naberezhnov, Yu. A. Kumzerov, I. V. Golosovsky, and A. S. Ivanov, JETP **111**, 996 (2010).

[8] P. P. Parshin, M. G. Zemlyanov, G. Kh. Panova, A. A. Shikov, Yu. A. Kumzerov, A. A. Naberezhnov, I. Sergueev, W. Crichton, A. I. Chumakov, and R. Rüffer, JETP **114**, 440 (2012).

[9]P. Villars, in *Pearson's Handbook: Desk Edition: Crystallographic Data for Intermetallic Phases* (ASM International, Materials Park, 1998).
[10]C. Tien, C. S. Wur, K. J. Lin, J. S. Hwang, E. V. Charnaya, and Yu. A. Kumzerov, Phys. Rev. B **54**, 11880 (1996).
[11]E. V. Charnaya, C. Tien, K. J. Lin, C. S. Wur, and Yu. A. Kumzerov, Phys. Rev. B **58**, 467 (1998).
[12]E. V. Charnaya, C. Tien, M. K. Lee, and Yu. A. Kumzerov, J. Phys.: Condens. Matter **21**, 455304 (2009).
[13]I. G. Sorina, E. V. Charnaya, L. A. Smirnov, Yu. A. Kumzerov, and C. Tien, Phys. Solid State **40**, 1407 (1998).
[14]M. K. Lee, C. Tien, E. V. Charnaya, H.-S. Sheu, and Yu. A. Kumzerov, Phys. Lett. A **374**, 1570 (2010).
[15]L. Bosio, A. Defrain, H. Curien, and A. Rimsky, Acta Crystallogr. Sect. B **25**, 995 (1969).
[16]A. D. DiCicco, Phys. Rev. Lett. **81**, 2942 (1998).
[17]Z. Liu, Y. Bando, M. Mitome, and J. Zhan, Phys. Rev. Lett. **93**, 095504 (2004).
[18]A. A. Bossak and Y. A. Kibalin, the synchrotron radiation experiments with gallium nanoparticles within a porous glass with 7 nm pore size and sample size of about 100 μm revealed the tetragonal structure with space group $I4/mmm$ and the unit cell parameters 3.2243(4) and 4.873(1) Å. (unpublished).
[19]H. Parr and J. Feder, Phys. Rev. B **7**, 166 (1973).
[20]E. V. Charnaya, Yu. A. Kumzerov, C. Tien, and C. S. Wur, Solid State Commun. **94**, 635 (1995).
[21]E. V. Charnaya, C. Tien, C. S. Wur, and Yu. A. Kumzerov, Physica C **269**, 313 (1996).
[22]P. Levitz, G. Ehret, S. K. Sinha, and J. M. Drake, J. Chem. Phys. **95**, 6151 (1991).
[23]P. Fischer, G. Frey, M. Koch, M. Könnecke, V. Pomjakushin, J. Schefer, R. Thut, N. Schlumpf, R. Bürge, U. Greuter, S. Bondt, and E. Berruyer, Physica B **276-278**, 146 (2000).
[24]W. A. Reed and J. A. Marcus, Phys. Rev. **130**, 957 (1963).
[25]H. J. Bunge, in *Texture Analysis in Materials Science* (Butterworth-Heinemann, London, 1998).
[26]S. Matthies, G. W. Vinel, and K. Helming, in *Standard Distributions in Texture Analysis* (Akademie, Berlin, 1987).
[27]H. M. Rietveld, J. Appl. Crystallogr. **2**, 65 (1969).
[28]M. Ferrari and L. Lutterotti, J. Appl. Phys. **76**, 7246 (1994).
[29]P. Thompson, D. Cox, and B. Hastings, J. Appl. Crystallogr. **20**, 79 (1987).
[30]B. T. Willis and A. W. Pryor, in *Thermal Vibration in Crystallography* (Cambridge University Press, Cambridge, 1974).
[31]H. Wenzl and G. Mair, Z. Phys. B **21**, 95 (1975).
[32]P. P. Parshin (private communication).
[33]N. Phillips, Phys. Rev. B **134**, A385 (1964).
[34]R. D. Horning and J.-L. Staudenmann, Acta Crystallogr. Sect. A **44**, 136 (1988).
[35]A. V. Marchenko, Glass Phys. Chem. **34**, 255 (2008).
[36]G. Kh. Panova, A. A. Naberezhnov, and A. V. Fokin, Phys. Solid State **50**, 1370 (2008).
[37]E. Grüneisen, Handb. Phys. **10**, 1 (1926).
[38]I. Suzuki, S.-I. Okajima, and K. Seya, J. Phys. Earth **27**, 63 (1979).
[39]J.-P. Poirier, in *Introduction to the Physics of the Earth's Interior*, 2nd ed. (Cambridge University Press, Cambridge, 2000).
[40]C. J. Smithells, in *Smithell Metals Reference Book*, 7th ed., edited by E. A. Brandes and G. B. Brook (Elsevier, New York, 1998).
[41]R. Griessen, H. Krugman, and H. R. Ott, Phys. Rev. B **10**, 1160 (1974).
[42]H. R. Ott and R. S. Sorbello, J. Low Temp. Phys. **14**, 73 (1974).
[43]A. P. Babichev *et al*., in *Handbook of Physical Quantities*, edited by I. S. Grigoriev and E. Z. Meylihova (Energoatomizdat, Moscow, 1991) (in Russian).
[44]W. Assmus *et al*., in *Springer Handbook of Condensed Matter and Materials Data*, edited by W. Martienssen and W. Warlimont (Springer, Berlin, 2005).
[45]Y. Kikuchi, H. Sudo, and N. Kuzuu, J. Appl. Phys. **82**, 4121 (1997).
[46]I. V. Golosovsky, M. Tovar, U. Hoffman, I. Mirebeau, F. Fauth, D. A. Kurdyukov, and Yu. A. Kumzerov, JETP Lett. **83**, 298 (2006).
[47]The enhanced nanoparticle size with respect to the pore size is a general phenomenon for confined nanoparticles and explained by the crystallization in the adjacent pores.
[48]This procedure is similar to the restoring of the pair correlation function.